Progress In Electromagnetics Research C, Vol. 99, 35–48, 2020

Microstrip Defected Ground Structure for Determination of Blood Glucose Concentration

S. K. Yee[1, *], S. C. J. Lim[2], P. S. Pong[1], and SH. Dahlan[1]

Abstract—This work reports the application of a microwave sensor in measuring human blood glucose concentration. The main contribution of this work lies on the blood glucose profile which is collected from 69 random patients regardless of their gender, age, and haematology properties, instead of using water as the base or focusing on a single person. Hence the blood glucose profile is more realistic. Blood is extracted from the participants and dropped at the centre of the dumbbells section of a microstrip defected ground structure to gather the notch frequency shifting data. On the other hand, the blood samples are measured using Omron Freestyle Glucometer to collect their associated blood glucose readings. Five predicting models have been proposed in this work. Based on the cross-validation, it is found that the blood glucose level can be correlated very well with shifted notch frequency by using a linear model. It introduces least root mean square error (RMSE) of 0.0592 and shows good correlation ($R^2 = 0.9356$) between the reading from commercial glucometer and microwave sensor in the range up to 12 mmol/L. The reliability of this microwave sensor is proven once again when the predicted blood glucose data are all falling in Zone A of Clarke Error Grid. The outcome of this work shows the capability of this microwave sensor in measuring the blood glucose level. Since this microwave sensor can be reused under a proper cleaning procedure, it improves the sustainability of conventional blood glucose testing by reducing the disposal of testing strips and cost. It is believed that this sensor will be suitable for extensive blood glucose testing conducted in the laboratory.

1. INTRODUCTION

Diabetes prevalence is one of the most broadly spread modern lifestyle diseases. According to the International Diabetes Federation in 2015, estimated 415 million people globally were suffering from this condition [1]. Diabetes is often associated with other complications such as skin infections, glaucoma, cataracts, kidney disease, stroke, high blood pressure, and diabetic neuropathy [2] and ranks among the leading causes of death globally. Currently, the medical treatments of diabetes are more towards appropriate medication, blood glucose level monitoring, and diet control.

Blood glucose supplies energy to the human body through bloodstream. This sugar exists in the body as the result of diet. Hence, it is strongly dependent on the food consumed as well as the ability of the body to regulate its level. The blood glucose is mainly contributed by foods that are rich in carbohydrates. When foods travel down to the stomach, acids and enzymes will break them down to small pieces; at this time, glucose is released. It continues to travel through the intestines, where it will be absorbed into the blood. The beta-cells in pancreas will monitor the blood sugar level and discharge insulin when the blood glucose rises after meal. Then, glucose is used along with amino acids and fats for energy production [3].

Received 5 November 2019, Accepted 6 January 2020, Scheduled 23 January 2020
* Corresponding author: See Khee Yee (skyste@gmail.com).
[1] Research Center for Applied Electromagnetics, Faculty of Electrical and Electronic Engineering, Universiti Tun Hussein Onn Malaysia, Malaysia. [2] Faculty of Technical and Vocational Education, Universiti Tun Hussein Onn Malaysia, Malaysia.

Usually, the blood glucose level varies throughout the day. When the body is in fasting regime, glucose levels in the bloodstream are relatively lower. According to [3], it should be less than 100 mg/dl for a healthy person. However, within 1–2 hours after meal, it should remain below 140 mg/dl. When the glucose level exceeds the normal range, the person is said to have diabetes. There are three common types of diabetes, namely Type 1, Type 2, and Gestational diabetes.

Type 1 diabetes (T1D) is a chronic autoimmune disease characterised by insulin deficiency, which is often linked to immune-associated destruction of pancreatic beta-cells, which produce insulin [4]. Historically, it is considered as a disorder in children and adolescents; however, this opinion has changed. Symptomatic onset is reported to be precipitated by genetic predisposition with an environmental trigger [5]. Virtually, Type 2 diabetes (T2D) is caused by insulin resistance, and prospective studies have shown that this insulin resistance has been long developed internally before the onset of this disease [6]. In this case, the pancreas still produces some insulin, but its amount is not adequate for the body's needs, or the body's cells are resistant to it [4]. Skeletal muscle and liver are the insulin-responsive organs responsible for maintaining normal glucose homeostasis, and their transition to an insulin-resistant state accounts for most of the alterations in glucose metabolism seen in patients with Type 2 diabetes [6]. Hence people who are suffering from obesity are at higher risk of Type 2 diabetes [4]. Gestational diabetes (GDM) is defined as glucose intolerance resulting in hyperglycaemia of variable severity with onset during pregnancy [7]. It frequently occurs in women with subclinical metabolic dysfunction before conception [8]. The metabolic dysfunction includes impaired insulin response, decreased hepatic suppression of glucose production during insulin infusion, and decreased insulin-stimulated glucose uptake in skeletal muscle [8]. It is reported that insulin sensitivity declines with advancing gestation for normal pregnancy due to placental factors, progesterone, and estrogen. It is mainly related to macrosomia caused by fetal hyperinsulinism in response to high glucose levels coming from maternal hyperglycemia [7]. Hence, additional insulin secretion happens to maintain normal glucose homeostasis. However when the pancreatic beta-cells are unable to cope with the insulin demand during the pregnancy, GDM occurs. Usually, women who are suffering from GDM are predisposed to Type 2 Diabetes (T2D).

Glucose monitoring devices or self-testing blood glucose meters had long existed during the 1980s. They are cost-effective electrochemical biosensors which are produced massively. They can respond rapidly to the glucose by relying on enzyme-electrode strips. Since an enzyme is used, it is particularly only for D-glucose and will not be subject to interferences from other molecules in the blood. The enzyme glucose oxidase catalyses the oxidation of Beta-D-glucose to D-gluconic acid. The Alpha-D-glucose is rapidly converted to the beta form so that all of the glucose is measured at one time [9]. When the strip is inserted into the glucometer, the flux of the glucose reaction generates an electrical signal [9], which is proportional to the glucose level. At present, these devices remain as the favourite of most of the consumers due to its portability, and its accuracy is clinically proven. However, frequent blood glucose monitoring based on this technique is a painful experience as it uses lancet devices to prick the fingertip for blood extraction. Furthermore, diabetic patients have to bear with the cost of strips and the boredom of making repeated measurement. Safety precautions during lancet disposal must be strictly followed to avoid danger during garbage handling.

As an effort to reduce the enzyme-electrode strips disposal, microwave sensors have been developed and used for glucose monitoring. Microwave sensing is a label-free technique which is based on the variation of capacitance and inductance as the result of electromagnetic interaction with the sample. The works in literature show that microwave sensors such as ring resonators [10], bandstop filter [11], complimentary split-ring resonator [12] and complementary electric-LC resonator [13] are appropriate for aqueous solution analysis. Besides that, in these works, the authors enhanced the sensitivity of the microwave sensor for glucose detection by introducing new elements [14] at the sensor or combine 2 microwave designs in one sensor [15]. For instance, they applied a layer of glucose oxidase enzyme at the sensing part of the sensor, since the enzyme only reacts with glucose. After the reaction, the frequency shifting is recorded for the prediction purpose. It is revealed that the variation of the glucose concentration affects the phase of the reflection and transmission coefficient (S_{11} and S_{21}) [10], resonant frequency shift [14], and normalized magnitude of S_{21} [11, 15]. A linear relationship is found in between variation of these microwave responses and glucose concentration.

More researches have been carried out extensively to invent a more compact, light weight, painless,

and noninvasive device for continuing blood glucose monitoring. They can be categorized as optical, transdermal, and thermal techniques [17]. Optical techniques rely on the interaction of infrared with glucose. When the radiation penetrates the tissue through skin, it is partially absorbed and scattered. On the other hand, transdermal method measures glucose concentration based on the ultrasound propagation through the skin. Lastly, thermal techniques measure the physiologic indices related to metabolic heat generation and local oxygen supply, which corresponds to the glucose concentration in the local blood supply [17].

RF and microwave sensors have been chosen as the technological platform for noninvasive blood glucose testing as it is believed to be a precise, safe, and fast technique which can provide continuous reading at the same time [18]. Many microstrip transmission line based schemes have been proposed as an electromagnetic sensor in previous works. A few designs have been proposed such as open terminated spiral shape microstrip line [19], microwave double split-ring resonator [18, 20–22], four spiral arms antenna [23], bandpass filter [24], microwave resonator with interdigital capacitor [25, 26], and dielectric probe [27] for detecting the variation of blood glucose. The working principle behind all these sensors lies on the deviation of complex permittivity with the presence of blood with fluctuation of glucose concentration [28]. The research findings show that the alteration in the blood glucose level can be reflected from measurement parameters such as transmission and reflection (S_{21} and S_{11}) [19, 23], the shifting of resonance frequency [18, 20–22], 3 dB bandwidth [18, 20–22], and standing wave ratio [19]. Since they are noninvasive techniques, the measurements are taken from the body parts. It is a challenging investigation because parameters such as body temperature [22], the pressure applied on the sensor as well as the position of the thumb [26] must be taken care to ensure measurement accuracy and repeatability. Since these sensors do not contact with the blood directly, the variation of dielectric property of skin, fat, muscle is studied based on simulation. It is highlighted that a slight change in the dielectric constant of skin will affect the resonance frequency shifting significantly [21], compared to other tissues such as fat and muscle. The findings from these studies are limited because there is lack of clinical testing. Furthermore, due to the limitation explained, they are either focused on the blood glucose level from a person after meals [22] or after oral glucose tolerance test [18]. In order to obtain wider range of blood glucose level, in-vitro testing is conducted [28].

Many noninvasive glucose monitoring devices are operated based on the techniques mentioned emerge, such as GlucoWatch®G2 Biographer, Pendra®, OrSense NBM-200G, C8 MediSensors [1, 17, 29]. Unfortunately, some of them are withdrawn from the market mainly due to accuracy and stability issues. The devices' accuracy is strongly dependent on physicochemical parameters such as body temperature, blood pressure, skin hydration, and environmental variation such as temperature and humidity. Besides that some of them are subject to errors due to sweating and motion. It is reported that some of the implanted amperometric biosensors [30] frequently require finger-stick validation, weekly device replacement, and suffer from potential of microbial infection and skin irritation. The risky consequences implicitly reduce its popularity in wide community. Hence, these minimal invasive devices cannot replace the traditional glucose meter completely. Consistent improvements on the algorithms, software, and device features are necessary to improve its user-friendliness, accuracy, and versatility.

This work intends to present a blood glucose detection technique based on a bandstop filter with defected ground structure (DGS) invasively. It is believed that invasive techniques are still a more reliable, safe, and robust method compared to non-invasive techniques which suffer from uncertainties contributed by body temperature, pressure, and position of the body parts, variation of dielectric properties of skin as well as lacking real case study. To the best of our knowledge, no microwave sensors use actual human blood to form the fundamental base of the blood glucose prediction. This technique does not utilize enzyme-electrode strips, despite that the blood is dropped on the sensor, and the same sensor can be reused again hence cut down the disposal of testing strips and cost. Therefore, it improves the sustainability of conventional blood glucose testing. In the following sections, the design of a sensor will be explained in detail, as well as the sample placement configuration. Next, the process regarding the data collection will be described. In the result and discussion section, the blood data will be presented together with the proposed predictive models. These models will be justified thoroughly from its accuracy and reliability aspect.

2. METHODOLOGY

This section of the paper describes a bandstop filter with a dumbbell defected ground structure (DGS) used in this work. It includes the blood sample placement as well as the process of data collection based on the sensors and commercial glucometer Omron Freestyle Glucometer.

2.1. Sensor Design

For this work, a bandstop filter with dumbbell defected ground structure (DGS) has been chosen as a sensor for predicting human blood glucose. DGS is a compact geometrical slot embedded on the ground plane of microwave circuits. FR-4 is used as the substrate while the microstrip trace and grounding are the copper strip. FR-4 is a grade designation assigned to glass-reinforced epoxy laminate sheets, tubes, rods, and printed circuit boards (PCBs). It is a composite material composed of woven fibreglass cloth with an epoxy resin binder that is flame resistant. The defects on the ground plane disturb the current distribution of the ground plane and hence change the effective capacitance and inductance of microstrip line by adding slot resistance, capacitance, and inductance [31]. Fig. 1 shows the view of the sensor from CST MICROWAVE STUDIO®(computer simulator) and its dimension.

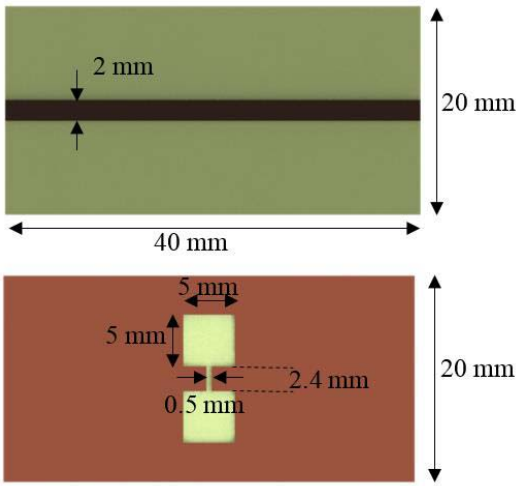

Figure 1. Front and back view of dumbbell DGS in CST MICROWAVE STUDIO®.

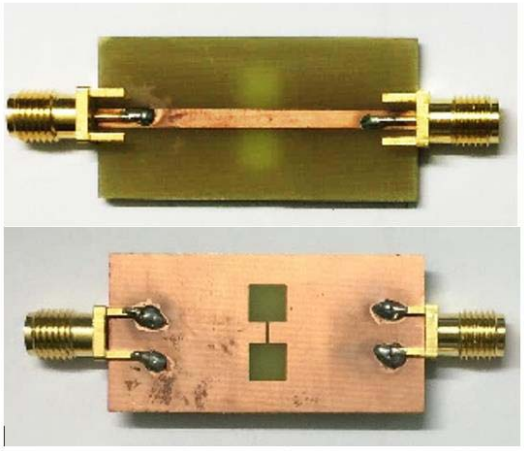

Figure 2. Actual dumbbell DGS soldered with SMA connectors.

The sensor is fabricated according to the standard etching process. A few sensor prototypes have been prepared. The one with the closest performance to the simulated results is chosen for blood glucose detection. The sensor is soldered with SMA connectors to facilitate its connection to the vector network analyzer (VNA). Fig. 2 shows the fabricated dumbbell DGSs soldered with SMA connector at both ends of the structure.

The notch frequency of the fabricated microwave sensor is measured by using the Rohde & Schwarz FSH4 spectrum analyzer which has the feature of VNA. The measured notch frequency is different from simulated notch frequency in some respects as tabulated in Table 1. Fig. 3 pictures S_{21} measurement

Table 1. Comparison of simulated and measured filter parameters.

	Notch frequency (GHz), α	3 dB bandwidth (GHz)	Q-factor	Amplitude of S_{21} (dB)
Simulation	5.94	0.473	12.56	−21.07
Measurement	6.31	0.3428	18.41	−24.73

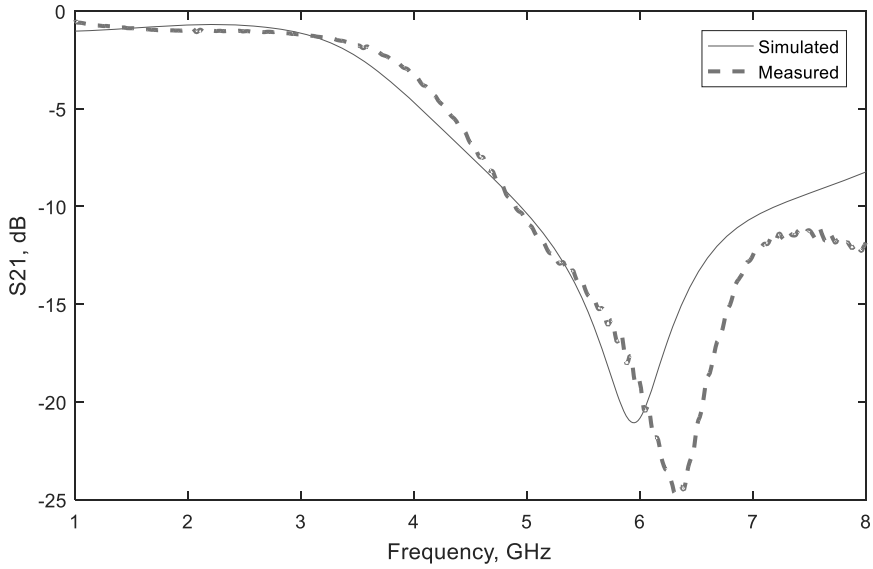

Figure 3. Comparison of simulated and measured notch frequency of dumbbell DGS.

comparison. The simulation result indicates the notch frequency of the sensor at 5.94 GHz; however, the actual notch frequency happens at 6.31 GHz. From the aspect of S_{21} amplitude, the simulated reading is higher (−21.07 dB) than the measured reading (−24.73 dB). The calculation indicates that the measured Q-factor is better than the simulated Q-factor. There are a few reasons that contribute to the discrepancy such as minor difference in the dimension in between virtual and actual structure, mismatching effect due to soldering of SMA connectors at the sensor as well as the minor tolerance of the permittivity and thickness of the substrate [32].

2.2. Sample Placement

As the sensor is connected to the VNA, energy is coupled into the sensors, and the S_{21} signal is captured. This parameter is strongly dependent on the dielectric properties such as relative permittivity and conductivity of the sample presents at the sensing part. Relative permittivity is a complex parameter where its real part is known as dielectric constant, and its imaginary part is named as loss factor. Dielectric constant describes the ability of a material to store the energy when being exposed to electric field while the loss factor measures the energy dissipated by the material when being exposed to electric field [32].

Based on the computer simulation, strong electric field distribution is found at the dumbells area located at the ground plane, as indicated in Fig. 4. This scenario indicates that the dumbell area is highly sensitive to the variation of dielectric properties of samples, and blood samples should be placed at this location. For the sake to reduce the amount of blood, further analysis and simulations are conducted. A smaller amount of blood is defined at four different positions of the dumbbells as shown in Fig. 5. Blood material has been chosen from the library of the simulator, and its thickness is fixed at 1 mm. The simulated notch frequency for each configuration is shown in Fig. 6.

Based on the comparison from Fig. 6, it is observed that by covering either one or both dumbbells ((c) and (b) configurations), both present the same S_{21} response. The blood sample has enhanced the magnitude of S_{21}, and the notch frequency is shifted significantly away from the notch frequency when no blood is placed at the dumbbells. Similar observation happens on configuration (d) as well. As for configuration (a), its S_{21} response is very similar to the original notch frequency except its notch frequency. It has been shifted slightly due to the introduction of blood sample. Hence, based on this analysis, configuration (a) will be chosen as the technique to drop the blood samples. The experimental configuration (a) is shown in Fig. 7 when it comes to data collection.

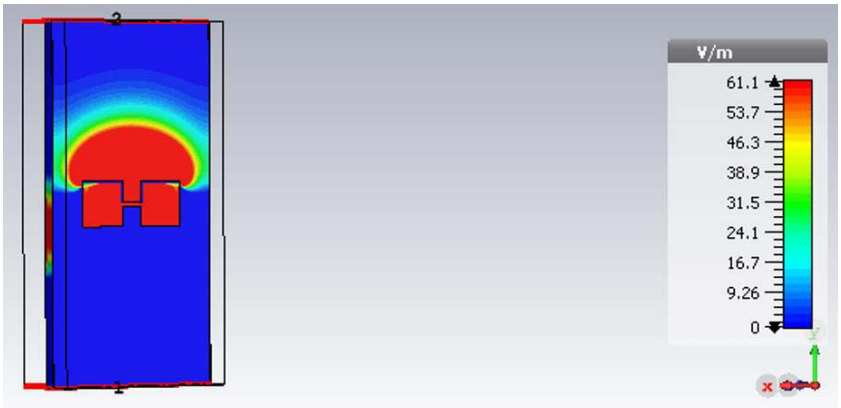

Figure 4. Electric field distribution at the dumbbell area based on computer simulation.

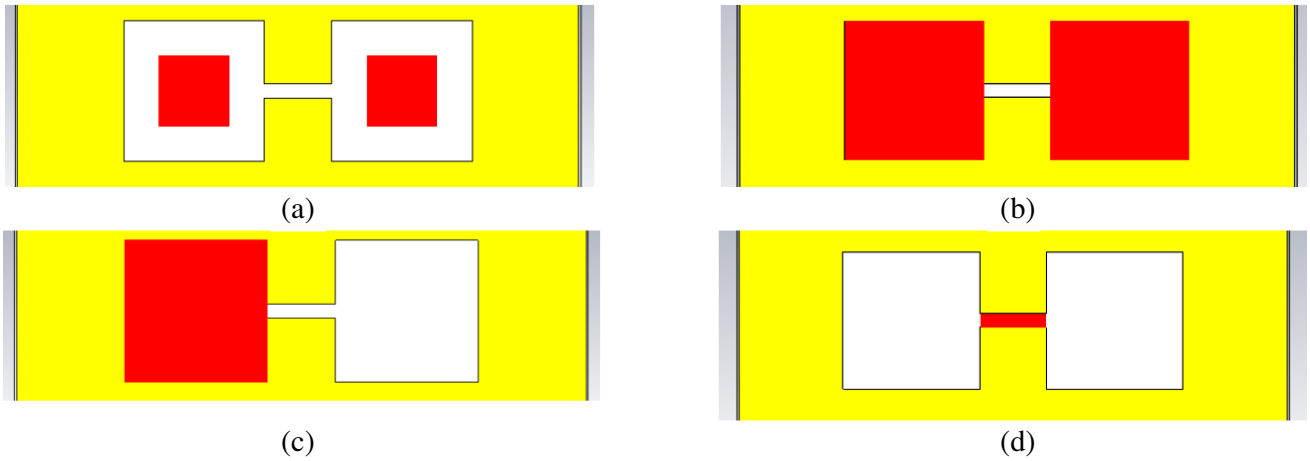

Figure 5. (a) Smaller portion of blood (red colour) is located at the centre of the dumbells. (b) The blood fully covers the dumbells. (c) The blood only covers 1 of the dumbells. (d) The blood covers the slot connecting both dumbells.

2.3. Data Collection

In this work, a total of 69 blood samples are collected from the University Health Center. These blood samples proceed with two tests. The first test is conducted using commercial Glucometer, Omron Freestyle Glucometer, which measures the blood glucose level in mmol/L. The test strip of the blood glucose meter is inserted to its port for activation. One drop of the blood sample is transferred to the test strips of glucometer, and the reading is recorded. The process of the measurement is shown in Fig. 8.

The second test is based on the proposed sensor in which the blood samples are dropped on the sensor as shown in Fig. 7. Two drops of blood samples are transferred to the dumbbell DGS by using pipette, and the notch frequency shifting is recorded. The measurement of the notch frequency shifting is repeated for thrice to ensure consistency and repeatability. Fig. 9 shows the testing procedures. The dumbbell DGS is cleaned by using alcohol swab after each measurement to ensure that it is well disinfected.

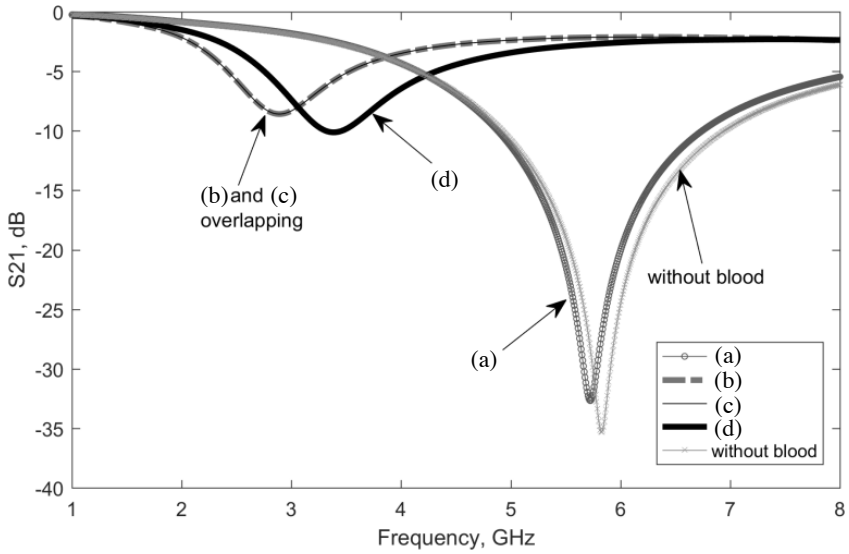

Figure 6. Comparison of the S_{21} (dB) when the blood sample is placed at different positions as indicated by Figure 5.

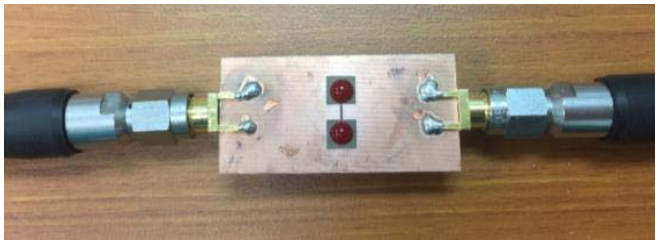

Figure 7. Actual configuration (a).

Figure 8. Measurement of blood glucose level by using Omron Freestyle Glucometer.

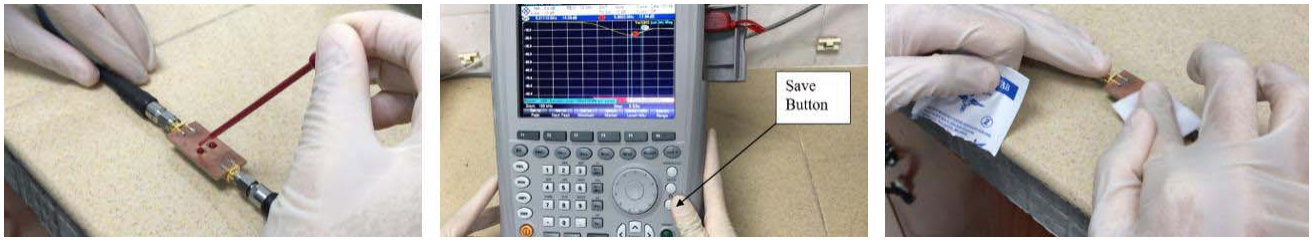

Figure 9. Collecting notch frequency shifting by using VNA.

3. RESULTS AND DISCUSSION

3.1. Data Preprocessing

This work applies invasive blood glucose monitoring based on a microwave sensor (bandstop filter with a defected-ground structure (DGS)). The notch frequency of this filter shall be shifted accordingly depending on the blood glucose level dropped on the sensing part of the DGS. When a blood sample is present, the notch frequency shift is witnessed experimentally. Mathematically, notch frequency shift can be defined as in Eq. (1), where f_n is the new notch frequency as the result of placing the blood sample, and α is regarded as the original notch frequency of the sensor. f_s is the difference between the new and original notch frequencies (shifted frequency).

$$f_s = f_n - \alpha \tag{1}$$

For every blood sample, notch frequency values were measured three times. As a result, a total of 69 sets of measurements were obtained. For each set of measurement, averaged notch frequency and shifted frequency values were determined. From the design of the sensor, the original notch frequency is determined to be $\alpha = 6.31$ GHz. Based on the averaged frequency values, a scatter plot using glucose concentration versus both frequency values has been performed, as shown in Fig. 10. In this study, the shifted frequency is chosen for further analysis due to the increasing trend of the graph, which resembles a logarithmic or exponential growth trend.

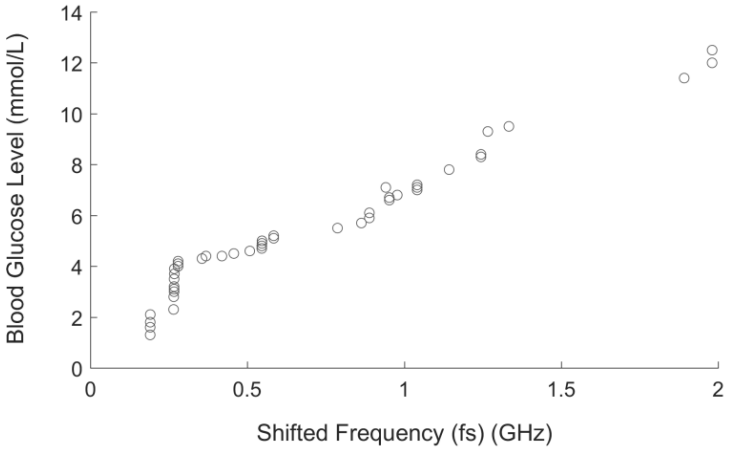

Figure 10. The blood glucose level (commercial glucometer) vs. shifted frequency (sensor proposed).

3.2. Predictive Modeling and Analysis

Based on the scatter plot as presented in Fig. 10, suitable predictive modelling is investigated further using a few regression models that may possibly capture the graph trend, namely: (1) Michaelis-Menten equation [33], (2) Linear-Log Regression Model, (3) Nonlinear Logistic Regression Model, and (4) Polynomial Cubic Regression Model (cubic). A simple linear regression model is also included as a Base Model. Details of the formulation for every model and the parameters involved are as summarized in Table 2.

Based on the $n = 69$ dataset, parameters for each of the models were determined. Table 3 summarises the results obtained, where estimated values and other related metrics are detailed. Graphically, a plot of every model is also added to the scatter plot as shown in Fig. 11. From Table 3, it is evident that the estimated values obtained are significant with very small p-value ($p < 0.001$), except three parameters for Model 4 where one of its parameters is significant within $p < 0.005$, and another two of its parameters are not significant with large p-values ($p > 0.05$). In comparison, such a result shows that the parameters of Model 4 are less significant. This may hint that the model is a less reliable

Table 2. Prediction models used in this work.

ID	Regression Model	General Formulation	Parameters
1	Michaelis-Menten	$y = \frac{ax}{b+x}$	a, b
2	Linear-Log	$y = a + b\ln(x)$	a, b
3	Nonlinear Logistic	$y = \frac{a}{1+e^{\frac{b-x}{c}}}$	a, b, c
4	Polynomial Cubic	$y = a + bx + cx^2 + dx^3$	a, b, c, d
Base	Linear	$y = a + bx$	a, b

Table 3. Parameter estimation for regression models.

Model	Parameter	Estimated	S. Error	t	$\Pr(>\|t\|)/p$-value
1	a	17.2540	1.3230	13.2450	2×10^{-16}
	b	1.2910	0.1590	8.1190	1.47×10^{-11}
2	a	7.5209	0.1496	50.26	2×10^{-16}
	b	3.300	0.1528	21.59	2×10^{-16}
3	a	15.4400	1.3986	11.0400	2×10^{-16}
	b	1.1070	0.1395	7.935	3.46×10^{-11}
	c	0.6825	0.0606	11.2700	2×10^{-16}
4	a	1.3725	0.4284	3.203	0.0021
	b	8.4785	1.9588	4.3280	5.3×10^{-5}
	c	-4.0635	2.2804	-1.782	0.0794
	d	1.2979	0.7274	1.7840	0.0791
Base	a	2.0640	0.1193	17.30	2×10^{-16}
	b	5.9774	0.1627	31.21	2×10^{-16}

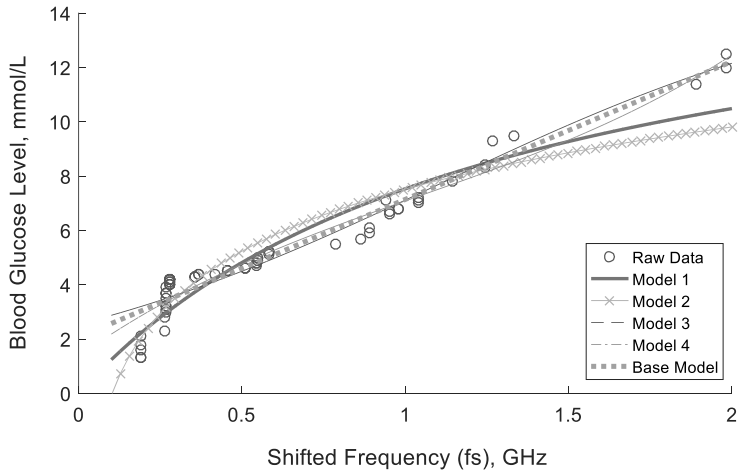

Figure 11. Comparison between the raw data and models fitting.

prediction model than other models, although the plot for this model in Fig. 11 seems reasonably fit. Nevertheless, this is not the only indicator for selecting the best model, and as a good prediction model it should have a small difference between a predicted value and the actual experimental value. As such, validation and selection of the best model will be presented in the next section.

3.3. Model Validation and Selection

For model validation, 5-fold and 10-fold cross-validations with 100 times repetition are performed. 5-fold cross-validation means that the dataset is randomly sub-divided into five subsets, with four subsets used for model training and the remaining one for prediction. Likewise, 10-fold cross-validation uses nine subsets of data for model training and the remaining one for prediction. In this study, as datasets are randomly sub-divided, the consistency of random dataset sub-division for every 100 times of repetition has been ensured.

For metrics, root mean square error (RMSE) has been applied as the selecting indicator, where it is the root-squared value of the averaged sum of squared differences (SSE) between model predicted values (y_p) and actual experimental values (y_a). Mathematically, it can be defined as Eqs. (2) and (3), with $n = 100$ in this study.

$$\text{RMSE} = \sqrt{\frac{\text{SSE}}{n}} \tag{2}$$

$$\text{SSE} = \sum_{i=1}^{n} y_p - y_a \tag{3}$$

The results of the cross-validation exercise for both 5-fold and 10-fold validation are as summarized in Table 4. From the table, most of the mean RMSE values are lower than 0.5, which is small

Table 4. Summary of results for cross-validation (RMSE).

Model ID	5-Fold		10-Fold	
	Mean	Standard Deviation	Mean	Standard Deviation
1	0.3528	0.0594	0.2490	0.0725
2	0.3706	0.0787	0.2575	0.0914
3	0.2664	0.0676	0.1880	0.0657
4	0.2638	0.0578	0.2686	0.6041
Base	0.2554	0.0598	0.1780	0.0592

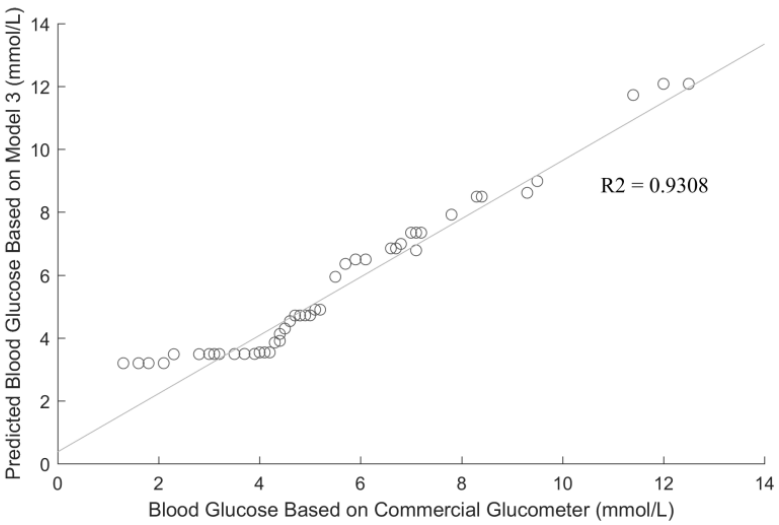

Figure 12. Scatter chart showing the predicted blood glucose concentration (Model 3) against the reference blood glucose concentration, showing an excellent positive correlation between these two data sets.

(RMSE < 1) and acceptable. In addition, the small standard deviation values indicate consistency of cross-validation outcome for 100 times repetitions. From the results, it is found that Base Model has the best performance with the lowest RMSE for both cross-validation experiments. Model 3 (Nonlinear Logistic Regression Model) comes close to the second-best, with around 5% performance difference compared to Base Model. Model 4 has the worst performance among all the models studied, possibly caused by the insignificant parameter values estimation. Overall, based on the available experimental data, Base Model and Model 3 are both suitable prediction models for blood glucose prediction based on notch frequency.

Figures 12 and 13 show the regression analysis of the predicted blood glucose level compared to the blood glucose level obtained from the commercial glucometer. When the data points are located perfectly on a linear line, the linear correlation coefficient, R^2, will be equal to 1. Based on the observation, the points are located close to the linear lines, and both models achieve linear correlation coefficient, R^2 above 0.9, which is very close to 1. This indicates that blood glucose data for the two models are closely related.

Between these two models, Base Model is found to have a better correlation with the actual

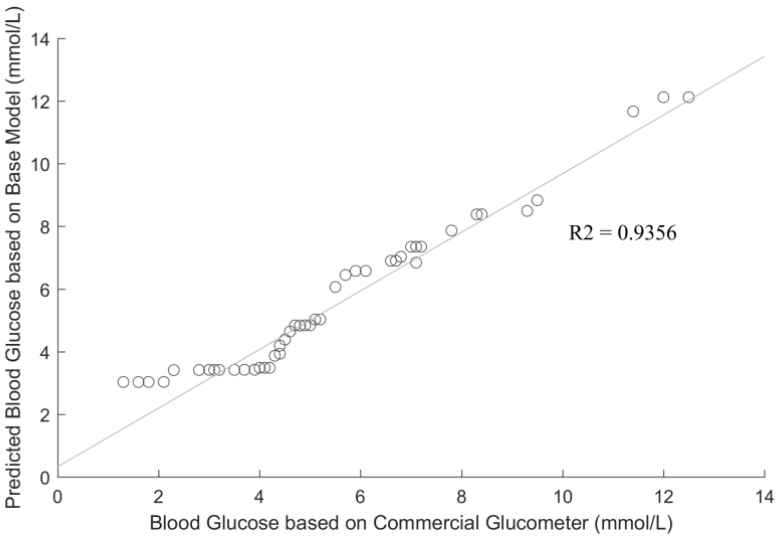

Figure 13. Scatter chart showing the predicted blood glucose concentration (Base Model) against the reference blood glucose concentration, showing an excellent positive correlation between these two data sets.

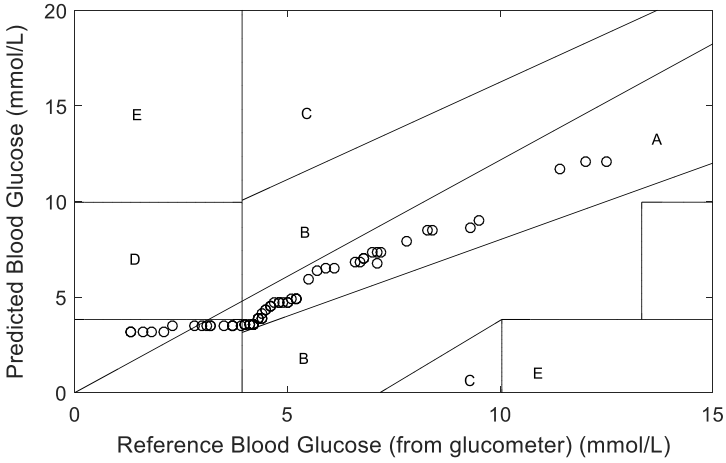

Figure 14. All the predicted blood glucose data is located in Zone A of Clarke Error Grid.

data since it has higher correlation coefficient, R^2. It is in agreement with the cross-validation results presented in Table 4. The predicted data based on Base Model is plotted in the Clarke Error Grid as shown in Fig. 14. Clarke Error Grid is used to quantify the clinical accuracy of blood glucose estimates generated by meters as compared to a reference value [34]. The x-axis represents the reference blood glucose while the y-axis is the value generated by the monitoring system (blood glucose prediction system). The diagonal straight line indicates a perfect matching between these two data points. The data points below or above the diagonal line represent the underestimation and overestimation of the data, respectively. It is split into five zones namely A, B, C, D, and E. When the values fall in Zone A, clinically correct decision will be conducted as the glucose values deviate from the reference by $< 20\%$. For Zone B, the values deviate from the reference by $> 20\%$, and this leads to clinically uncritical decisions. However, the data falling under Zones C, D, and E will lead to overcorrecting blood glucose treatment, skipping a necessary treatment and performing the opposite or wrong treatment, respectively. The predicted data by using Base Model fall perfectly in Zone A, and none of them are located in other zones. This indicates that if the proposed blood glucose sensor is used for diagnosis, it can lead to correct medical decisions or treatment. It once again proves the reliability of the prediction model and sensor.

4. CONCLUSIONS

This work has demonstrated a reliable microwave sensor for blood glucose measurement application by correlating with commercial handy Omron Freestyle Glucometer. A total of 69 participants have generated a blood dataset of 207 as the measurement is repeated thrice. The mean value of the notch frequency shifting has been used to establish the blood glucose profile of this work. Five models namely Michaelis-Mcnten (Model 1), Linear-Log (Model 2), Nonlinear Logistic (Model 3), Polynomial Cubic (Model 4), and Linear (Base Model) have been proposed as the predictive model to frame a relationship between the blood glucose level and notch frequency shifting. However, it is evident from the cross-validation, correlation coefficient, and Clarke error grid that predictive model based on Base Model is the best alternative as it introduces 0.0592 of RMSE in 10-fold cross-validation and 0.9356 of correlation coefficient. Furthermore, the predicted blood glucose level based on Base Model falls within Zone A in the Clarke error grid. The outcome of this work has validated the linear relationship between the glucose level and predicted parameters which are reported in previous works [13, 19, 35]. The extension and novelty of this work is its blood glucose profile formation based on actual blood samples from participants regardless of their gender, age, and haematology properties, such as total red blood count, total white blood count, and haemoglobin, instead of using water as the base or focusing on a single person. This work, therefore, shows the potential of a microwave sensor as a promising blood glucose sensor. Future works should focus on two primary areas, first, more data collection especially those blood glucose above nine mmol/L to improve the predictive model and second, the improvement for a complete blood glucose sensor system which is more handy and user-friendly (with computer interface).

ACKNOWLEDGMENT

The work described in this paper was partially supported by a research grant (Tier-1) by the Office of Research Innovation Commercialization and Consultancy Management (ORICC), Universiti Tun Hussein Onn Malaysia (Grant Ref: H231).

REFERENCES

1. Yacine, M., "Non-invasive glucose monitoring: Application and technologies," *Curr. Trends Biomed. Eng. Biosci.*, Vol. 14, No. 1, 1–6, 2019.
2. Bruen, D., C. Delaney, L. Florea, and D. Diamond, "Glucose sensing for diabetes monitoring: Recent developments," *Sensors (Switzerland)*, Vol. 17, No. 8, 1866, Aug. 2017.
3. James, P. and R. McFadden, "Understanding the processes behind the regulation of blood glucose," *Nursing Times*, Vol. 100, No. 16, 56–58, 2004.

4. Atkinson, M. A., G. S. Eisenbarth, and A. W. Michels, "Type 1 diabetes," *Lancet*, Vol. 383, No. 9911, 69–82, Jan. 2014.
5. Skyler, J. S., et al., "Differentiation of diabetes by pathophysiology, natural history, and prognosis," *Diabetes*, Vol. 66, No. 2, 241–255, 2017.
6. Parish, R. and K. F. Petersen, "Mitochondrial dysfunction and type 2 diabetes," *Curr. Diab. Rep.*, Vol. 5, No. 3, 177–183, Jun. 2005.
7. Baz, B., J. P. Riveline, and J. F. Gautier, "Gestational diabetes mellitus: Definition, aetiological and clinical aspects," *Eur. J. Endocrinol.*, Vol. 174, No. 2, R43–R51, 2016.
8. Catalano, P. M., "Trying to understand gestational diabetes," *Diabet. Med.*, Vol. 31, No. 3, 273–281, Mar. 2014.
9. Nery, E. W., M. Kundys, P. S. Jeleń, and M. Jönsson-Niedziólka, "Electrochemical glucose sensing: Is there still room for improvement?," *Anal. Chem.*, Vol. 88, No. 23, 11271–11282, Dec. 2016.
10. Schwerthoeffer, U., R. Weigel, and D. Kissinger, "A highly sensitive glucose biosensor based on a microstrip ring resonator," *2013 IEEE MTT-S International Microwave Workshop Series on RF and Wireless Technologies for Biomedical and Healthcare Applications, IMWS-BIO 2013 — Proceedings*, 2013.
11. Chretiennot, T., D. Dubuc, and K. Grenier, "Microwave-based microfluidic sensor for non-destructive and quantitative glucose monitoring in aqueous solution," *Sensors (Switzerland)*, Vol. 16, No. 10, 1733, 2016.
12. Mondal, D., N. K. Tiwari, and M. J. Akhtar, "Microwave assisted non-invasive microfluidic biosensor for monitoring glucose concentration," *Proceedings of IEEE Sensors*, Vol. 2018, Oct. 2018.
13. Ebrahimi, A., W. Withayachumnankul, S. F. Al-Sarawi, and D. Abbott, "Microwave microfluidic sensor for determination of glucose concentration in water," *Mediterranean Microwave Symposium*, Vol. 2015, Jan. 2015.
14. Camli, B., E. Kusakci, B. Lafci, S. Salman, H. Torun, and A. Yalcinkaya, "A microwave ring resonator based glucose sensor," *Procedia Engineering*, Vol. 168, 465–468, 2016.
15. Harnsoongnoen, S. and A. Wanthong, "Coplanar waveguide transmission line loaded with electric-LC resonator for determination of glucose concentration sensing," *IEEE Sens. J.*, Vol. 17, No. 6, 1635–1640, 2017.
16. Abedeen, Z. and P. Agarwal, "Microwave sensing technique based label-free and real-time planar glucose analyzer fabricated on FR4," *Sensors Actuators A: Phys.*, Vol. 279, 132–139, 2018.
17. Lin, T., "Non-invasive glucose monitoring: A review of challenges and recent advances," *Curr. Trends Biomed. Eng. Biosci.*, Vol. 6, No. 5, 2017.
18. Choi, H., et al., "Design and in vitro interference test of microwave noninvasive blood glucose monitoring sensor," *IEEE Trans. Microw. Theory Tech.*, Vol. 63, No. 10, 3016–3025, 2015.
19. Jean, B. R., E. C. Green, and M. J. McClung, "A microwave frequency sensor for non-invasive blood-glucose measurement," *2008 IEEE Sensors Applications Symposium, SAS-2008 — Proceedings*, 4–7, 2008.
20. Choi, H., S. Luzio, J. Beutler, and A. Porch, "Microwave noninvasive blood glucose monitoring sensor: Human clinical trial results," *IEEE MTT-S International Microwave Symposium Digest*, 876–879, 2017.
21. Choi, H., S. Luzio, J. Beutler, and A. Porch, "Microwave noninvasive blood glucose monitoring sensor: Penetration depth and sensitivity analysis," *IMBioc 2018 — 2018 IEEE/MTT-S International Microwave Biomedical Conference*, 52–54, 2018.
22. Choi, H., J. Nylon, S. Luzio, J. Beutler, and A. Porch, "Design of continuous non-invasive blood glucose monitoring sensor based on a microwave split ring resonator," *Conference Proceedings — 2014 IEEE MTT-S International Microwave Workshop Series on: RF and Wireless Technologies for Biomedical and Healthcare Applications, IMWS-Bio 2014*, 2015.
23. Shao, J., F. Yang, F. Xia, Q. Zhang, and Y. Chen, "A novel miniature spiral sensor for non-invasive blood glucose monitoring," *2016 10th European Conference on Antennas and Propagation, EuCAP 2016*, 2016.

24. Baghbani, R., M. A. Rad, and A. Pourziad, "Microwave sensor for non-invasive glucose measurements design and implementation of a novel linear," *IET Wirel. Sens. Syst.*, Vol. 5, No. 2, 51–57, Apr. 2015.
25. Turgul, V. and I. Kale, "Influence of fingerprints and finger positioning on accuracy of RF blood glucose measurement from fingertips," *Electron. Lett.*, Vol. 53, No. 4, 218–220, Feb. 2017.
26. Turgul, V. and I. Kale, "A novel pressure sensing circuit for non-invasive RF/microwave blood glucose sensors," *Mediterranean Microwave Symposium*, 2017.
27. Nakamura, M., T. Tajima, M. Seyama, and K. Waki, "A noninvasive blood glucose measurement by microwave dielectric spectroscopy: Drift correction technique," *IMBioc 2018 — 2018 IEEE/MTT-S International Microwave Biomedical Conference*, 85–87, 2018.
28. Karacolak, T., E. C. Moreland, and E. Topsakal, "Cole-cole model for glucose-dependent dielectric properties of blood plasma for continuous glucose monitoring," *Microw. Opt. Technol. Lett.*, Vol. 55, No. 5, 1160–1164, May 2013.
29. Wang, H. C. and A. R. Lee, "Recent developments in blood glucose sensors," *J. Food Drug Anal.*, Vol. 23, No. 2, 191–200, Jun. 2015.
30. Kim, J., A. S. Campbell, and J. Wang, "Wearable non-invasive epidermal glucose sensors: A review," *Talanta*, Vol. 177, 163–170, Jan. 2018.
31. Khandelwal, M. K., B. K. Kanaujia, and S. Kumar, "Defected ground structure: Fundamentals, analysis, and applications in modern wireless trends," *Int. J. Antennas Propag.*, Vol. 2017, 1–22, 2017.
32. Pozar, D. M., *Microwave Engineering*, Wiley, 2012.
33. Johnson, K. A. and R. S. Goody, "The original Michaelis constant: Translation of the 1913 Michaelis-Menten Paper," *Biochemistry*, Vol. 50, No. 39, 8264–8269, Oct. 2011.
34. Clarke, W. L., "The original clarke error grid analysis (EGA)," *Diabetes Technology and Therapeutics*, Vol. 7, No. 5, 776–779, 2005.
35. Vrba, J., D. Vrba, L. Díaz, and O. Fišer, "Metamaterial sensor for microwave non-invasive blood glucose monitoring," *IFMBE Proceedings*, Vol. 68, No. 3, 789–792, 2019.